

DOI: 10.1002/cbic.201402003

Investigation of Binding-Site Homology between Mushroom and Bacterial Tyrosinases by Using Aurones as Effectors

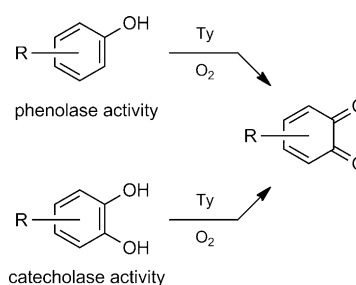
Romain Haudecoeur,^[a] Aurélie Gouron,^[b] Carole Dubois,^[c] Hélène Jamet,^[b] Mark Lightbody,^[a] Renaud Hardré,^[c] Anne Milet,^[b] Elisabetta Bergantino,^[d] Luigi Bubacco,^[d] Catherine Belle,^[b] Marius Réglie,^[c] and Ahcène Boumendjel^{*[a]}

Tyrosinase is a copper-containing enzyme found in plants and bacteria, as well as in humans, where it is involved in the biosynthesis of melanin-type pigments. Tyrosinase inhibitors have attracted remarkable research interest as whitening agents in cosmetology, antibrowning agents in food chemistry, and as therapeutics. In this context, commercially available tyrosinase from mushroom (TyM) is frequently used for the identification of inhibitors. This and bacterial tyrosinase (TyB) have been the subjects of intense biochemical and structural studies, including X-ray diffraction analysis, and this has led to the identification of structural homology and divergence among enzymes from different sources. To better understand the behavior of

potential inhibitors of TyM and TyB, we selected the aurone family—previously identified as potential inhibitors of melanin biosynthesis in human melanocytes. In this study, a series of 24 aurones with different hydroxylation patterns at the A- and B-rings were evaluated on TyM and TyB. The results show that, depending on the hydroxylation pattern of A- and B-rings, aurones can behave as inhibitors, substrates, and activators of both enzymes. Computational analysis was performed to identify residues surrounding the aurones in the active sites of both enzymes and to rationalize the interactions. Our results highlight similarities and divergence in the behavior of TyM and TyB toward the same set of molecules.

Introduction

Tyrosinases (Ty, EC 1.14.18.1) are metalloenzymes found in mammals, plants, fungi, and bacteria, and play critical roles in melanin pigment biosynthesis.^[1] Ty belongs to the type-3 copper-containing enzymes, characterized by a coupled binuclear active site that accepts phenols and catechols as substrates (Scheme 1).^[2,3] In humans, Ty is responsible for the two-step oxidation of L-tyrosine to dopaquinone: 1) hydroxylation of L-tyrosine to L-3,4-dihydroxyphenylalanine (L-DOPA), and 2) subsequent oxidation to *ortho*-quinone (dopaquinone). The latter undergoes further transformations through several polymerization steps to form melanin, the primary determinant of



Scheme 1. Reactions catalyzed by tyrosinases.

skin color. Ty also plays protective roles against UV radiation and oxidants, and in enzymatic hydrolysis, antimicrobials and phagocytosis. In bacteria, Ty was reported to be involved in several processes, such as pathogenic virulence and redox processes.^[4] In fungi and plants, Ty is a key enzyme in the browning process that occurs upon tissues damage and long term storage of fruit and vegetables.

In terms of structure–function relationship, low homology in sequence alignments (Table S1, Figures S1–S2 in the Supporting Information) between tyrosinases from different origins, suggests important differences in 3D structure, and therefore in functional behavior. These structural differences were highlighted by recent solutions of the crystallographic structures of different Ty forms. Because of the difficulties in producing human Ty (TyH) in high quantities by heterologous expression (see the Supporting Information), its 3D structure is still un-

[a] Dr. R. Haudecoeur,⁺ M. Lightbody, Prof. A. Boumendjel⁺⁺
Univ. Grenoble Alpes/CNRS, DPM UMR 5063
38041 Grenoble (France)
E-mail: Ahcene.Boumendjel@ujf-grenoble.fr

[b] A. Gouron,⁺ Dr. H. Jamet, Prof. A. Milet, Dr. C. Belle
Univ. Grenoble Alpes/CNRS, DCM UMR 5250
38041 Grenoble (France)

[c] Dr. C. Dubois,⁺ Dr. R. Hardré, Dr. M. Réglie⁺⁺
Aix-Marseille Université, Centrale Marseille, CNRS, ISM2 UMR 7313
13397 Marseille (France)

[d] Dr. E. Bergantino, Prof. L. Bubacco
Department of Biology, University of Padova
Via Ugo Bassi 58b, Padova, 35121 (Italy)

[⁺] These authors contributed equally to this work.

[⁺⁺] Both senior investigators contributed equally to this work.

Supporting information for this article is available on the WWW under <http://dx.doi.org/10.1002/cbic.201402003>.

known. In the last decade, the X-ray structures of two bacterial Ty forms (TyB1 from *Bacillus megaterium*^[5] and TyB2 from *Streptomyces castaneoglobisporus*)^[6] and two mushroom forms (TyM1 from *Agaricus bisporus*^[7] and TyM2 from *Aspergillus oryzae*)^[8] were solved. TyM1 crystallized as an H2L2 (two heavy, two light subunits) tetramer, including the copper-containing subunit H (392 residues), whereas TyM2 and the bacterial counterparts TyB1 and TyB2 crystallized as homodimers (620, 568, and 273 residues, respectively). In these three enzymes, the active site includes two copper atoms, each coordinated by three histidine residues (Figure 1). In both TyM1 and TyM2,

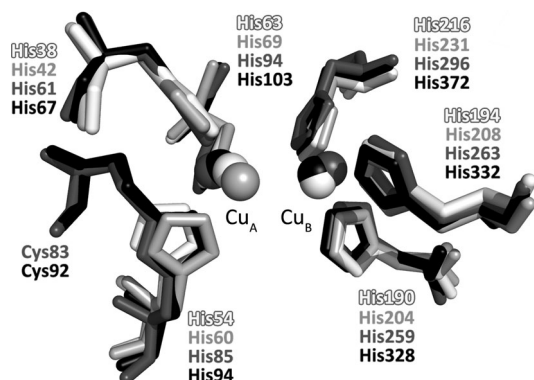


Figure 1. Superimposition of active sites of TyB1 (light gray), TyB2 (white), TyM1 (dark grey) and TyM2 (black).

one histidine residue (His85 and His94, respectively) is linked by a thioether bond to the side chain of a cysteine residue (Cys83 and Cys92, respectively), a feature not shared by TyB1 or TyB2 (where the active site is fairly well conserved). On the other hand, the second coordination spheres seem to differ considerably: only 58.3% identity for residues within 6 Å of the two copper atoms in superimposed structures of TyM1 and TyB2 (Figure S2).

The medical and economical impact of tyrosinase inhibitors are attested by the increasing number of compounds described recently.^[9] In humans, accumulation of high levels of melanin causes a variety of disorders, such as cutaneous hyperpigmentation (solar lentigo, melasma, naevi, etc.) and ocular retinitis pigmentosa.^[10] Also, Ty might be involved in Parkinson's disease development, through degradation of L-DOPA.^[11] In cosmetology, attention is focused on the development of tyrosinase inhibitors as skin-whitening agents by silencing melanin formation.^[12,13] In the food industry, tyrosinase inhibition (to reduce melanin synthesis) is being developed to control browning of fruit and vegetables.^[14–16]

Most tyrosinase inhibitors were developed by using commercially available mushroom tyrosinase (TyM) as a model, under the assumption of similarity between TyM and other tyrosinases. This assumption is rather hazardous because of the low sequence homology between Tys of different origin and differences in the binding pocket topologies, as recently reported for TyB^[5,6] and TyM.^[7,8] Consequentially, it can be hypothesized that a particular inhibitor might behave differently

with Tys from different sources (e.g., natural plant extracts, as reported very recently).^[17] In order to investigate this hypothesis, we studied the behavior of a series of compounds with Ty from mushroom and bacterial sources.

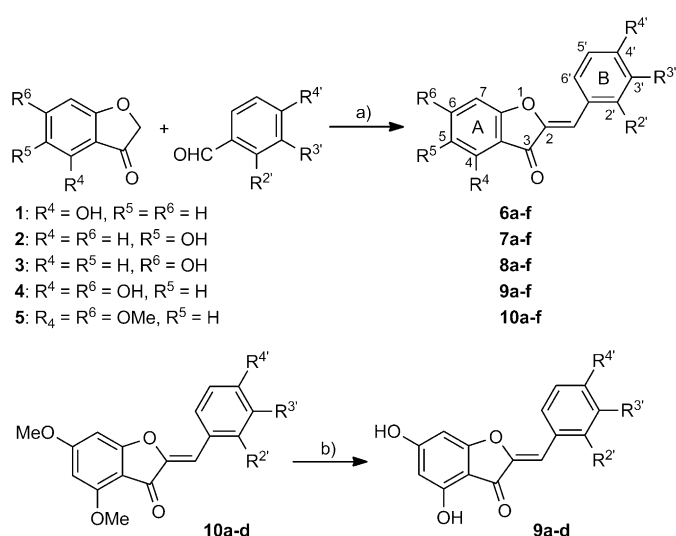
Previously, we reported that aurones (benzylidenebenzofuran-3(2*H*)-ones) are inhibitors of melanin biosynthesis in human melanocytes.^[18] Aurones are naturally occurring compounds of the flavonoid family, distributed across the plant kingdom, and their therapeutic potential is emerging.^[19,20] The effects of aurones on melanogenesis encouraged us to evaluate their action on the catalysis of mushroom and bacterial tyrosinases. For this, we compared the activities of *A. bisporus* tyrosinase (TyM1) and *Streptomyces antibioticus* tyrosinase (TyB3). The choice of TyB3 was motivated by our expertise in its expression and purification.^[21] In addition, TyB2 and TyB3 belong to the same *Streptomyces* genus and share more than 82% identity (Table S1).

Herein, we report the synthesis of a systematic library of polyhydroxylated aurones and the in vitro biological evaluation of this library against TyM1 and TyB3. The interactions between both Ty forms with aurones were analyzed and rationalized by computational analysis.

Results and Discussion

Synthesis

The synthesis of aurones was accomplished according to Scheme 2.^[20a] Typically, hydroxylated aurones were obtained from hydroxybenzofuran-3(2*H*)-one derivatives (1–5) through aldol condensation with commercially available benzaldehydes, by one of three procedures: basic KOH conditions in methanol at 65 °C, for aurones bearing up to one hydroxyl group per ring (6*b*–8*b*, 6*c*–8*c*, 6*d*–8*d*; procedure A); more concentrated KOH conditions in ethanol at 80 °C, for aurones bearing more than one hydroxyl group per ring (6*e*–8*e*, 6*f*–8*f*, 9; procedure



Scheme 2. Procedure A: a) KOH/H₂O, MeOH, 65 °C, 1–18 h. Procedure B: a) KOH/H₂O, EtOH, 80 °C, 2–5 h; b) BBr₃, CH₂Cl₂, 0 °C to RT, 24–72 h. Procedure C: a) H₂SO₄, MeOH, 65 °C.

B); and acidic stoichiometric H₂SO₄ conditions in methanol at 65 °C, for 4,6,4'-trihydroxyaurone (**9d**; procedure C). Some 4,6-dihydroxyaurones (**9**) were obtained from the corresponding 4,6-dimethoxyaurones (**10**), by demethylation with boron tribromide in CH₂Cl₂.^[20a]

Structure–activity relationships

Our previous study with a few aurone members (6-hydroxyaurones, Table 1, **8a–e**) highlighted the extraordinary versatile effects of the aurone structure on TyM1 activity.^[22] Although the B-unsubstituted aurone (**8a**) was found to be inactive, 4'-hydroxyaurones (**8d** and **8e**) behaved as alternative substrates and were converted by TyM1 into *ortho*-quinone, thereby demonstrating that aurones interact at their B-ring with the dinuclear copper–oxygen active site. In contrast, 3'- and 2'-hydroxyaurones (**8b** and **8c**) behaved as activators. An important feature pointed out in our previous study is the likely occurrence of multiple binding sites on TyM1 for aurones.^[22] In the present study, we compared the behavior of TyM1 and TyB3 toward a larger library of aurones: those with diversely hydroxylated A- and B-rings. Tyrosinase inactivation by resorcinols was recently reported; this prompted us to include **6f–9f**, which contain resorcinol moieties at the B-ring.^[23] For TyM1, we used a commercially available *A. bisporus* Ty, purified by Q-sepharose FF chromatography according to a known procedure.^[24] The *S. antibioticus* TyB3 was produced in the strain *S. antibioticus* pLJ703 and purified according to a published procedure.^[21] For both enzymes, we determined the Michaelis–Menten kinetic parameters for L-DOPA oxidation by plotting absorbance at

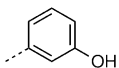
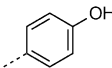
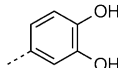
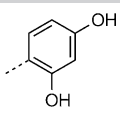
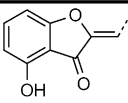
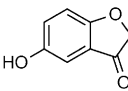
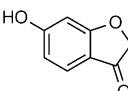
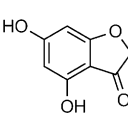
475 nm against time (formation of DOPochrome). For TyM1, $K_m = (0.39 \pm 0.04) \text{ mM}$, $v_{\text{max}} = (0.48 \pm 0.01) \mu\text{M s}^{-1}$ (ref. [25]: $K_m = (0.6 \pm 0.15) \text{ mM}$; $v_{\text{max}} = 0.38 \mu\text{M s}^{-1}$) and for TyB3, $K_m = (2.4 \pm 0.7) \text{ mM}$, $v_{\text{max}} = (45 \pm 4) \mu\text{M s}^{-1}$.

For substrate behavior, the enzymatic kinetics were determined by monitoring the disappearance of the large band presented by the aurones in the UV–visible spectra (~400 nm, adjusted for each substrate; Table S4). For activator activity, activities in absence or presence of aurones were compared at saturating concentrations of L-DOPA (2.8 mM) followed by classical analysis (plotting $1/v_{\text{app}}$ against reciprocal activator concentration).^[26] For inhibitors, we verified first that Ty inhibition is concentration-dependent, and determined IC₅₀ values at 1.25 mM L-DOPA.

The previously reported values for aurones **8a–8e** with TyM1 (discussed above)^[22] were fully reflected for other aurones. Regardless the A-ring substitution, the general behavior associated with the B-ring substitution remained similar. In all cases, an unsubstituted B-ring led to inactive compounds; 2'-hydroxy- (**6b–9b**) and 3'-hydroxyaurones (**6c–9c**) were TyM1 activators (Table 2); 4'-hydroxy- (**6d–9d**) and 3',4'-dihydroxyaurones (**6e–9e**) were identified as alternative TyM1 substrates (Table 3).

The second important discovery was that aurones have different reactivities toward TyM1 and TyB3. The main differences were observed with 2'-hydroxy- (**6b–9b**) and 3'-hydroxyaurones (**6c–9c**). Although **6b–9b** and **6c–9c** exhibited activation of TyM1, they behaved as poor inhibitors of TyB3 (Table 2). This difference can be explained by the significant differences in the structures of TyM1 and TyB3. Unlike TyBs, which are mono-

Table 1. Activity of aurones (A, activator; I, inhibitor; S, substrate; n.a., no activity; n.d., not determined).

												
	TyM1	TyB3	TyM1	TyB3	TyM1	TyB3	TyM1	TyB3	TyM1	TyB3	TyM1	TyB3
	6a	6b	6c	6d	6e	6f						
	n.a.	n.a.	A	I*	A	I*	S***	S***	S**	n.d.	I***	I***
	7a	7b	7c	7d	7e	7f						
	n.a.	n.a.	A	I*	A	I*	S**	S**	S**	n.d.	I*	I**
	8a	8b	8c	8d	8e	8f						
	n.a.	n.a.	A	I*	A	I*	S***	S***	S*	S*	I*	I**
	9a	9b	9c	9d	9e	9f						
	n.a.	n.a.	A	I**	A	I**	S***	S****	S**	S****	I**	I***

**** Very high activity (K_m or $IC_{50} \leq 1 \mu\text{M}$). *** High activity ($20 \mu\text{M} \geq K_m$ or $IC_{50} > 1 \mu\text{M}$). ** Moderate activity ($200 \mu\text{M} \geq K_m$ or $IC_{50} > 20 \mu\text{M}$). * Low activity ($1 \text{ mM} \geq K_m$ or $IC_{50} > 200 \mu\text{M}$).

Table 2. Hyperbolic activation (H.A.) values and IC_{50} determined for compounds **6b–9b** and **6c–9c** against TyM1 and TyB3.

Compound	R ⁴	R ⁵	R ⁶	R ^{2'}	R ^{3'}	TyM1 H.A. [%]	TyB3 IC_{50} [μ M]
6b	OH	H	H	OH	H	200	400 ± 20
7b	H	OH	H	OH	H	120	450 ± 100
8b	H	H	OH	OH	H	120	> 1000
9b	OH	H	OH	OH	H	180	150 ± 25
6c	OH	H	H	H	OH	170	> 400
7c	H	OH	H	H	OH	150	700 ± 100
8c	H	H	OH	H	OH	240	> 1000
9c	OH	H	OH	H	OH	150	> 200

$K_m = 52.9 \mu\text{M}$) to poor activity (**8e**, $K_m = 288 \mu\text{M}$), whereas (as for **9d**), the 4,6-disubstituted aurone (**9e**) was a very efficient substrate for TyB3 ($K_m = 1 \mu\text{M}$).

Finally, 2',4'-dihydroxyaurones (resorcinol-based aurones, **6f–9f**) behaved as inhibitors of both enzymes (Tables 1 and 4), but with significant IC_{50} variation. For TyM1, 2',4,4'-trihydroxyaurone (**6f**) behaved as

meric in solution, TyM1 is obtained as a heterodimer of a heavy subunit (containing the active center) and a light subunit.

For the other aurones, the activities were similar. A substrate or inhibitor for TyM1 behaved similarly toward TyB3. The differences lay in the range of activities. For example, the 4'-hydroxyaurones (**6d–9d**) showed the same reactivity for both Tys; they behaved as substrates for both enzymes (Table 3). However some K_m differences were observed, depending on the A-ring substitution. Introduction of a hydroxy substituent at the 5-position (**7d**) induced a negative effect on K_m ; **7d** was found to be a bad substrate for TyM1 ($K_m = 170 \mu\text{M}$) and TyB3 ($K_m = 79 \mu\text{M}$). Regarding hydroxylation of positions 4 and 6, both hydroxy aurones constituted good substrates for TyM1 (**6d**, $K_m = 5 \mu\text{M}$; **8d**, $K_m = 4.8 \mu\text{M}$) and TyB3 (**6d**, $K_m = 10 \mu\text{M}$; **8d**, $K_m = 9 \mu\text{M}$). Interestingly, the 4,6-dihydroxy aurone (**9d**) showed increased K_m with TyM1 ($K_m = 18.2 \mu\text{M}$), but decreased K_m (by two orders of magnitude) with TyB3 ($K_m = 0.2 \mu\text{M}$), compared to monosubstituted aurones **6d** and **8d**. For 3',4'-dihydroxy aurones (catechol-based aurones, **6e–9e**), the hydroxylation effect was less clear. With TyM1, **6e–9e** exhibited average (**6e**, $K_m = 51 \mu\text{M}$; **7e**, $K_m = 53 \mu\text{M}$, **9e**,

Table 4. Inhibition constants and IC_{50} values with standard deviations determined for compounds **6f–9f** against TyM1 and TyB3.

Compound	R ⁴	R ⁵	R ⁶	R ^{2'}	R ^{4'}	TyM1 IC_{50} [μ M]	TyB3 IC_{50} [μ M]
6f	OH	H	H	OH	OH	9 ± 1	4 ± 1
7f	H	OH	H	OH	OH	> 1000	62 ± 12
8f	H	H	OH	OH	OH	> 1000	100 ± 10
9f	OH	H	OH	OH	OH	300 ± 20	18 ± 3

a good inhibitor ($IC_{50} = 9 \mu\text{M}$) whereas the 2',4,4',6-tetrahydroxyaurone (**9f**) showed weaker activity ($IC_{50} = 300 \mu\text{M}$). Monosubstituted 5- and 6-aurones (**7f** and **8f**) displayed almost no activity ($IC_{50} > 1 \text{ mM}$). For TyB3, the tendency observed with substrates **6d–9d** was conserved. The best inhibitor was the 4,6-disubstituted aurone (**9f**, $IC_{50} = 18 \mu\text{M}$), noticeably better than the 4- and 6-substituted counterparts (**6f**, $IC_{50} = 100 \mu\text{M}$, **8f**, $IC_{50} = 100 \mu\text{M}$). Collectively, these results reveal distinct variability in interaction of these aurones with TyM1 and TyB3.

Aurone–Ty complexes: interaction studies using quantum and molecular mechanics studies

To rationalize the interactions between the aurones and the two Ty enzymes, dynamics coupling quantum and molecular mechanics (QM/MM) were performed. Calculations were con-

Table 3. Michaelis constants and maximum reaction rates with standard deviations determined for compounds **6d–9d** and **6e–9e** against TyM1 and TyB3 (n.d., not determined).

Compound									
	R ⁴	R ⁵	R ⁶	R ^{2'}	R ^{3'}	TyM1	TyB3		
						K_m [μ M]	v_{app} [$\mu\text{M min}^{-1}$]	K_m [μ M]	v_{app} [$\mu\text{M min}^{-1}$]
6d	OH	H	H	H	OH	5 ± 1	0.046 ± 0.003	10 ± 3	0.10 ± 0.01
7d	H	OH	H	H	OH	170 ± 50	0.56 ± 0.09	79 ± 14	0.42 ± 0.06
8d	H	H	OH	H	OH	4.8 ± 0.1	3.0 ± 0.3	9 ± 2	0.63 ± 0.05
9d	OH	H	OH	H	OH	18.2 ± 0.1	2.4 ± 0.6	0.20 ± 0.08	6.7 ± 0.8
6e	OH	H	H	OH	OH	51 ± 12	7.1 ± 0.6	n.d.	n.d.
7e	H	OH	H	OH	OH	53 ± 5	25 ± 3	n.d.	n.d.
8e	H	H	OH	OH	OH	288 ± 10	91 ± 8	300 ± 200	6.1 ± 0.7
9e	OH	H	OH	OH	OH	52.9 ± 0.3	39 ± 5	1.0 ± 0.3	0.36 ± 0.05

ducted with **6f**, **8f**, and **9f** (Table 4), which showed the greatest contrast in IC_{50} values. Estimation of the binding free energies of aurone–Ty complexes was computed with the inclusion of solvation effects through Poisson–Boltzmann/surface area calculations, namely QM/MM-PBSA.^[27–29] This approach provided valuable information for better identification of the residues surrounding the aurones in both Tys. Similar MM evaluation was performed on the docked positions of thujaplicins with a homology model of TyM.^[30] In our case, aurones **6f**, **8f**, and **9f** are competitive inhibitors, so their interaction with the copper atoms of the active site had to be incorporated into the theoretical calculations for QM analysis.

For TyM1, calculations were performed with the recent X-ray structure.^[7] In the absence of an X-ray structure of TyB3, these calculations were performed by using crystallographic data for TyB2 (>82% identity to TyB3; Table S1).^[6] For the aurone, the choice and the construction of the initial position in the active site are detailed in Computational Methods (below). QM/MM geometry optimizations of the aurone–Ty complexes were performed. For each enzyme, the optimized structures for the three inhibitors in the active site were found to be very close, and this cannot explain the experimentally observed differences between the three ligands in terms of activity. Then protein flexibility was considered, by computing short QM/MM dynamics for the six complexes. These simulations did not identify major structural differences at the active site and similar copper–copper (3.5–3.9 Å), copper–ligand (1.9–2.1 Å), and copper–water (2.0–2.4 Å) distances were observed. But several differences were observed for the interactions with neighboring active-site residues. Specifically, if no major differences were identified between TyB2 complexes, we were able to highlight key interactions for TyM1; this allowed efficient discrimination of the three studied inhibitors.

For TyM1, the calculated binding free energies (QM/MM-PBSA) matched the experimental order of inhibition efficiency (**6f** > **9f** > **8f**, Figure 2). Several components of these energies (Table S2) were analyzed to identify residues contributing the most. Some residues in the second coordination sphere of the active site (2.5–4 Å from the ligand) led to favorable van der Waals effects. The major contributions for these interactions were from Phe264 and Val283, but Asn260, Val248, and His263 also had an effect (Figure 2). Compounds **6f** and **9f** seemed to be more buried in the binding pocket than **8f**. For **6f**, the most important feature was Phe264, rotation of which places the plane of the aromatic ring parallel to the five-membered ring of the aurone, whereas it is perpendicular to five-membered rings of **8f** and **9f**. The weak interactions with Val248 seemed to contribute more in the case of **9f** than for **6f** and **8f**. Residues Asn260, His263, and Arg268 displayed electrostatic effects on the ligands. In the case of **8f**, very weak interactions were found between Arg268 and the hydroxyl group at position 6 (6.7 Å), and the inhibitor was experimentally determined to be inactive ($\Delta G_{\text{calcd}} = 6.1 \text{ kcal mol}^{-1}$). For compound **9f**, Arg268 seemed to interact more strongly with the phenol group at position 4 of the aurone (2.7 Å), in agreement with its inhibitory activity ($IC_{50} = 300 \mu\text{M}$; $\Delta G_{\text{calcd}} = 3.9 \text{ kcal mol}^{-1}$). In both complexes, the arginine was not shifted and led to di-

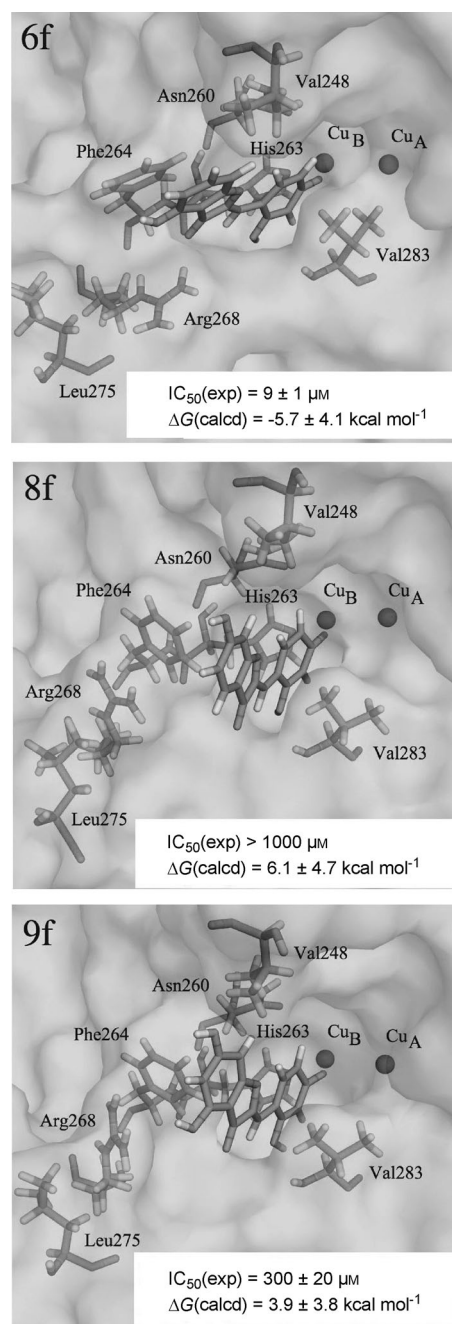


Figure 2. Snapshots from the MD trajectory of TyM1–aurone complexes.

hedral angles $C\alpha$ – $C\beta$ – $C\gamma$ – $C\delta$ of -160° to -180° . Interestingly, in the case of **6f**, Arg268 underwent a rotation ($C\alpha$ – $C\beta$ – $C\gamma$ – $C\delta$ 130 to 140°) and shifted to build a hydrogen bond with the carbonyl of aurone and some weaker electrostatic interactions with the phenol at position 4 (3.9 Å). This motion was allowed because of the absence of 6-hydroxyl group in the case of **6f**, whereas **8f** and **9f** bear this substituent. Additionally, the arginine was stabilized in this position through the formation of an extra hydrogen bond with the main chain of adjacent Leu275 (1.9 Å). All these elements contributed to a strengthened inhibitory effect of TyM1 ($IC_{50} = 9 \mu\text{M}$; $\Delta G_{\text{calcd}} = -5.7 \text{ kcal mol}^{-1}$).

For TyB2, although binding affinities ΔG_{calcd} seemed to follow the experimental order of inhibition efficiency, high standard deviation values prevented us from drawing a clear rational conclusion from these calculations (Table S3). Additionally, no major differences were identified in the interactions between the three inhibitors and the neighboring active-site residues, even after QM/MM dynamics. However the calculations enabled us to identify the hot-spot residues for TyB2 and to highlight divergences from TyM1. In TyB2, the main van der Waals and electrostatic contributions arose from residues Ile42, Asn191, and Trp183. The aurones also seemed to stand at the edge of the binding pocket (5 Å from Val195; Figure 3). Hence, their A-rings allowed much less interaction with the protein

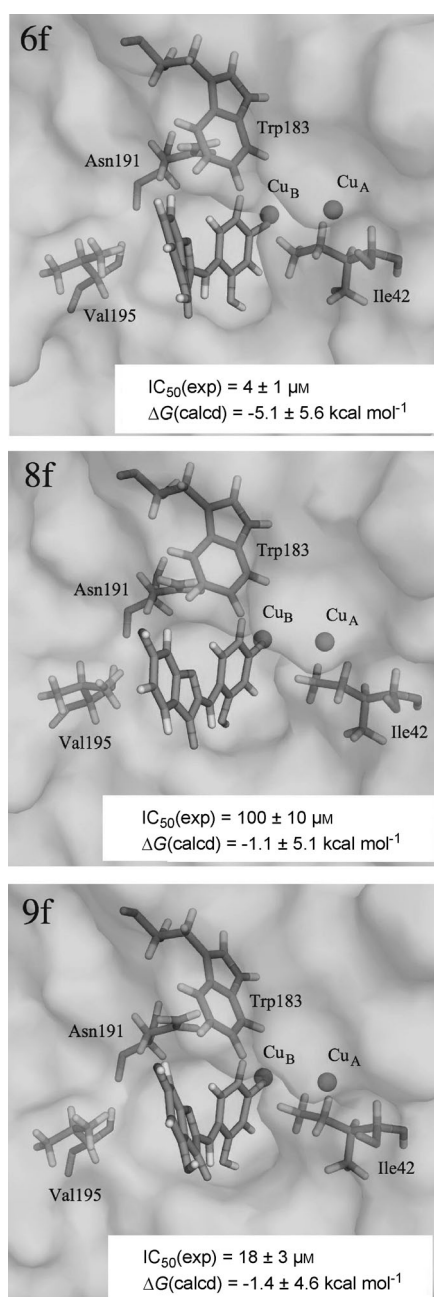


Figure 3. Snapshots from the MD trajectory of TyB2-aurone complexes.

residues than for TyM1, and, logically, van der Waals contributions in TyB2 were significantly lower.

A brief comparison between TyB2 and TyM1 crystallographic structures provided a first glimpse of similarities and differences between their active sites. The residues surrounding the aurones in TyB2 and TyM1 were identified after performing QM/MM dynamics on aurone-Ty complexes. Superimposition of the structures revealed that residues at 6 Å from the two copper centers and aurones in the structures exhibit only 28.6% identity (see the Supporting Information). The analysis of interactions between Ty and aurones highlighted the similarly positioned hot-spot residues in TyM1 and TyB2, especially Ile42/Val283, Val195/Phe264, Asn191/Asn260, and Trp183/Val248 (for TyB2/TyM1). Thus, their contributions to the respective interaction patterns appeared to diverge. Finally, the extensively interacting residue Arg268 of TyM1 was missing in the case of TyB2. This divergence constitutes one of the keys for affinity variability for the three aurones 6f, 8f, and 9f.

Conclusions

Aurones were investigated as ligands of tyrosinases from two sources (mushroom and bacteria) with the aim of better understanding the behavior of both enzymes toward the same compounds. The synthesis of 24 diversely hydroxylated aurones allowed us to identify common and divergent reactivity profiles toward bacterial and mushroom tyrosinases, TyB3 and TyM1. Substrate, activator, and inhibitor activities were found. The behavior and efficiency strongly depend on the A- and B-ring hydroxylation patterns, as well as on the enzyme origin. 2',4'-Dihydroxyaurones (resorcinol-like aurones) were identified as inhibitors of both TyM1 (IC_{50} = 9–1000 μM) and TyB3 (IC_{50} = 18–100 μM), with a high degree of potency. The QM/MM calculations on the complexes between inhibitors derived from aurones and TyM1 or TyB2 allowed us to identify key interactions and to highlight divergences between the two enzymes. In TyM1, we identified some residues to explain the differences in inhibition efficiency, such as Arg268, which can form a hydrogen bond with the carbonyl of some aurones. The second sphere of coordination of the active site is very poorly conserved between TyM1 and TyB2. Analysis of the computed interaction energies showed that the residues of the binding pockets interact differently with aurones.

These results suggest that different modes of binding and action of aurones occur, and that the different behaviors could be relevant to human tyrosinase. The main conclusion reached in this study is that inhibitors discovered by using TyM are not automatically effective for Tys from other origins, and that caution should thus be exercised.

Experimental Section

Chemistry: ^1H and ^{13}C NMR spectra were recorded on an AC-400 instrument (Bruker; 400 MHz for ^1H , 100 MHz for ^{13}C). Chemical shifts are reported in ppm relative to Me_4Si (internal standard). Electrospray ionization (ESI) mass spectra were acquired at the Analytical Department of Grenoble University on an Esquire 300 Plus

instrument (Bruker Daltonics) with a nanospray inlet. Combustion analyses were performed at the Analytical Department of Grenoble University; all tested compounds had a purity of at least 95%. Silica gel F-254 plates (0.25 mm; Merck) were used for thin-layer chromatography (TLC), and silica gel 60 (200–400 mesh; Merck) was used for flash chromatography. All solvents were distilled prior to use. Unless otherwise stated, reagents were obtained from commercial sources and were used without further purification. The synthesis of **1–5**, **6 f**, **7 d**, **8a–8d**, **9a–9b**, **9d–9f**, and **10a–10d** is as previously reported.^[20a]

Preparation of (Z)-2-benzylidenebenzofuran-3(2H)-one derivatives (procedure A): Aqueous potassium hydroxide (50%, 1.5 mL mmol⁻¹) and a benzaldehyde derivative (1.5 equiv) were added to a solution of a benzofuran-3(2H)-one derivative in methanol (15 mL mmol⁻¹). The solution was then refluxed until TLC showed complete disappearance of the starting material (1–18 h). After cooling, the mixture was concentrated under reduced pressure, then the residue was diluted in water (50 mL mmol⁻¹), and aqueous hydrochloric acid (1 M) was added (to pH 2–3). The mixture was extracted with ethyl acetate or dichloromethane and washed with water and brine. The combined organic layers were dried over magnesium sulfate and filtered, and the filtrate was concentrated under reduced pressure to give the crude compound.

Preparation of (Z)-2-benzylidenebenzofuran-3(2H)-one derivatives (procedure B): Aqueous potassium hydroxide (50%, 5 mL mmol⁻¹) and a benzaldehyde derivative (2 equiv) were added to benzofuran-3(2H)-one derivative in ethanol (4 mL mmol⁻¹). The solution was then refluxed until TLC showed complete disappearance of the starting materials (2–5 h). After cooling, the mixture was concentrated under reduced pressure, then the residue was diluted in water (50 mL mmol⁻¹), and aqueous hydrochloric acid (1 M) was added (to pH 2–3). The mixture was extracted with ethyl acetate or dichloromethane and washed with water and brine. The combined organic layers were dried over magnesium sulfate and filtered, and the filtrate was concentrated under reduced pressure to give the crude compound.

(Z)-2-(3,4-dihydroxybenzylidene)-4-hydroxybenzofuran-3(2H)-one (6e): The compound was prepared according to procedure B, starting from 4-hydroxybenzofuran-3(2H)-one (**1**) and 3,4-dihydroxybenzaldehyde, and was purified by column chromatography on silica gel eluted with CH₂Cl₂/MeOH (9:1) to yield a pure yellow solid (43%). M.p. >260 °C (decomposition); ¹H NMR (400 MHz, [D₆]DMSO): δ = 11.04 (brs, 1H; OH), 9.68 (brs, 1H; OH), 9.30 (brs, 1H; OH), 7.53 (t, *J* = 8.2 Hz, 1H; H₆), 7.46 (d, *J* = 1.9 Hz, 1H; H₂'), 7.26 (dd, *J*₁ = 8.4 Hz, *J*₂ = 1.9 Hz, 1H; H₆'), 6.84 (m, 2H; H₇, H₅'), 6.63 (d, *J* = 8.2 Hz, 1H; H₅), 6.63 ppm (s, 1H; –CH=); ¹³C NMR (100 MHz, [D₆]DMSO): δ = 181.0, 165.7, 156.9, 147.9, 145.5, 144.8, 138.1, 124.5, 123.4, 117.8, 116.0, 111.5, 110.3, 109.4, 102.3 ppm; MS (ESI): *m/z* 269 [M–H]⁻.

(Z)-2-benzylidene-5-hydroxybenzofuran-3(2H)-one (7a): The compound was prepared according to procedure A, starting from 5-hydroxybenzofuran-3(2H)-one (**2**) and benzaldehyde, and was purified by column chromatography on silica gel eluted with CH₂Cl₂/MeOH (9:1) to yield a pure yellow solid (10%). M.p. 216–218 °C; ¹H NMR (400 MHz, [D₆]DMSO): δ = 9.83 (brs, 1H, OH), 7.98 (d, *J* = 7.3 Hz, 2H; H₂', H₆'), 7.49 (m, 3H; H₃', H₄', H₅'), 7.41 (d, *J* = 8.8 Hz, 1H; H₆), 7.23 (dd, *J*₁ = 8.8 Hz, *J*₂ = 2.6 Hz, 1H; H₇), 7.03 (d, *J* = 2.6 Hz, 1H; H₄), 6.89 ppm (s, 1H; –CH=); ¹³C NMR (100 MHz, [D₆]DMSO): δ = 185.5, 160.9, 155.5, 148.7, 133.6, 132.8, 131.5, 130.5, 127.4, 122.7, 115.4, 113.2, 109.3 ppm; MS (ESI): *m/z* 239 [M+H]⁺.

(Z)-2-(2-hydroxybenzylidene)-5-hydroxybenzofuran-3(2H)-one (7b): The compound was prepared according to procedure A, starting from 5-hydroxybenzofuran-3(2H)-one (**2**) and 2-hydroxybenzaldehyde, and was purified by column chromatography on silica gel eluted with CH₂Cl₂/MeOH (9:1) to yield a pure yellow solid (88%). M.p. >230 °C (decomposition); ¹H NMR (400 MHz, [D₆]DMSO): δ = 10.36 (brs, 1H; OH), 9.77 (brs, 1H; OH), 8.12 (d, *J* = 7.7 Hz, 1H; H₆'), 7.39 (d, *J* = 8.6 Hz, 1H; H₆), 7.28 (t, *J* = 7.7 Hz, 1H; H₄'), 7.21 (d, *J* = 8.6 Hz, 1H; H₇), 7.19 (s, 1H; –CH=), 7.02 (s, 1H; H₄), 6.95 ppm (m, 2H; H₃', H₅'); ¹³C NMR (100 MHz, [D₆]DMSO): δ = 183.7, 159.1, 157.4, 153.8, 146.7, 131.7, 131.1, 125.5, 121.4, 119.7, 118.8, 115.8, 113.9, 107.7, 106.0 ppm; MS (ESI): *m/z* 255 [M+H]⁺, 277 [M+Na]⁺.

(Z)-2-(3-hydroxybenzylidene)-5-hydroxybenzofuran-3(2H)-one (7c): The compound was prepared according to procedure A, starting from 5-hydroxybenzofuran-3(2H)-one (**2**) and 3-hydroxybenzaldehyde, and was purified by column chromatography on silica gel eluted with CH₂Cl₂/MeOH (9:1) to yield a pure yellow solid (73%). M.p. >230 °C (decomposition); ¹H NMR (400 MHz, [D₆]DMSO): δ = 9.80 (brs, 1H; OH), 9.68 (brs, 1H; OH), 7.39 (m, 3H; H₆, H₂', H₆'), 7.29 (t, *J* = 7.8 Hz, 1H; H₅'), 7.23 (dd, *J*₁ = 8.8 Hz, *J*₂ = 2.6 Hz, 1H; H₇), 7.03 (d, *J* = 2.6 Hz, 1H; H₄), 6.86 (dd, *J*₁ = 7.8 Hz, *J*₂ = 1.9 Hz, 1H; H₄'), 6.78 ppm (s, 1H; –CH=); ¹³C NMR (100 MHz, [D₆]DMSO): δ = 183.9, 159.3, 157.6, 153.9, 147.0, 133.1, 129.9, 125.8, 122.6, 121.2, 117.5, 117.4, 113.8, 112.0, 107.8 ppm; MS (ESI): *m/z* 255 [M+H]⁺, 277 [M+Na]⁺.

(Z)-2-(3,4-hydroxybenzylidene)-5-hydroxybenzofuran-3(2H)-one (7e): The compound was prepared according to procedure B, starting from 5-hydroxybenzofuran-3(2H)-one (**2**) and 3,4-dihydroxybenzaldehyde, and was purified by column chromatography on silica gel eluted with CH₂Cl₂/MeOH (9:1) to yield a pure yellow solid (15%). M.p. >300 °C (decomposition). ¹H NMR (400 MHz, [D₆]DMSO): δ = 9.73 (brs, 2H; OH), 9.29 (brs, 1H; OH), 7.47 (d, *J* = 2.0 Hz, 1H; H₂'), 7.34 (d, *J* = 8.8 Hz, 1H; H₆), 7.29 (dd, *J*₁ = 8.4 Hz, *J*₂ = 2.0 Hz, 1H; H₆'), 7.20 (dd, *J*₁ = 8.8 Hz, *J*₂ = 2.7 Hz, 1H; H₇), 7.00 (d, *J* = 2.7 Hz, 1H; H₄), 6.84 (d, *J* = 8.4 Hz, 1H; H₅'), 6.73 ppm (s, 1H; –CH=); ¹³C NMR (100 MHz, [D₆]DMSO): δ = 183.4, 158.8, 153.7, 148.4, 145.6, 145.5, 125.3, 125.0, 123.4, 121.7, 118.1, 116.0, 113.6, 113.4, 107.6 ppm; MS (ESI): *m/z* 271 [M+H]⁺, 293 [M+Na]⁺.

(Z)-2-(2,4-hydroxybenzylidene)-5-hydroxybenzofuran-3(2H)-one (7f): The compound was prepared according to procedure B, starting from 5-hydroxybenzofuran-3(2H)-one (**2**) and 2,4-dihydroxybenzaldehyde, and was purified by column chromatography on silica gel eluted with CH₂Cl₂/MeOH (9:1) to yield a pure yellow solid (88%). M.p. >300 °C (decomposition); ¹H NMR (400 MHz, [D₆]DMSO): δ = 10.05 (brs, 3H; OH), 7.98 (d, *J* = 8.5 Hz, 1H; H₆'), 7.34 (d, *J* = 8.8 Hz, 1H; H₆), 7.17 (s, 1H; –CH=), 7.16 (dd, *J*₁ = 8.8 Hz, *J*₂ = 2.7 Hz, 1H; H₇), 6.99 (d, *J* = 2.7 Hz, 1H; H₄), 6.37 ppm (m, 2H; H₃', H₅'); ¹³C NMR (100 MHz, [D₆]DMSO): δ = 182.9, 161.8, 160.2, 158.4, 153.6, 144.8, 132.6, 124.8, 122.0, 113.6, 110.5, 108.4, 107.9, 107.4, 102.4 ppm; MS (ESI): *m/z* 271 [M+H]⁺, 293 [M+Na]⁺.

(Z)-2-(3,4-dihydroxybenzylidene)-6-hydroxybenzofuran-3(2H)-one (8e, sulfuretin): The compound was prepared according to procedure B, starting from 6-hydroxybenzofuran-3(2H)-one (**3**) and 3,4-dihydroxybenzaldehyde, and was purified by column chromatography on silica gel eluted with CH₂Cl₂/MeOH (9:1) to yield a pure yellow solid (26%). ¹H NMR (400 MHz, [D₆]DMSO): δ = 9.69 (brs, 3H; OH), 7.58 (d, *J* = 8.4 Hz, 1H; H₄), 7.44 (d, *J* = 1.9 Hz, 1H; H₂'), 7.24 (dd, *J*₁ = 8.2 Hz, *J*₂ = 1.9 Hz, 1H; H₆'), 6.83 (d, *J* = 8.2 Hz, 1H; H₅'), 6.72 (d, *J* = 1.7 Hz, 1H; H₇), 6.68 (dd, *J*₁ = 8.4 Hz, *J*₂ = 1.7 Hz, 1H; H₅), 6.62 ppm (s, 1H; –CH=); ¹³C NMR (100 MHz,

[D₆]DMSO): δ = 181.1, 167.4, 166.3, 148.0, 145.6, 145.5, 125.7, 124.5, 123.4, 117.9, 116.0, 113.1, 112.9, 111.8, 98.3 ppm; MS (ESI): m/z 271 [M+H]⁺.

(Z)-2-(2,4-dihydroxybenzylidene)-6-hydroxybenzofuran-3(2H)-one (8f): The compound was prepared according to procedure B, starting from 6-hydroxybenzofuran-3(2H)-one (3) and 2,4-dihydroxybenzaldehyde, and was purified by column chromatography on silica gel eluted with CH₂Cl₂/MeOH (9:1) to yield a pure red solid (72%). M.p. > 230 °C (decomposition); ¹H NMR (400 MHz, [D₆]DMSO): δ = 10.24 (brs, 3H; OH), 7.97 (d, J = 8.5 Hz, 1H; H6'), 7.57 (d, J = 8.4 Hz, 1H; H4), 7.05 (s, 1H; -CH=), 6.74 (d, J = 1.7 Hz, 1H; H7), 6.68 (dd, J_1 = 8.4 Hz, J_2 = 1.7 Hz, 1H; H5), 6.38–6.42 ppm (m, 2H; H3', H5'); ¹³C NMR (100 MHz, [D₆]DMSO): δ = 181.0, 167.2, 166.3, 160.8, 159.1, 145.1, 132.4, 125.5, 113.2, 112.8, 110.5, 108.3, 105.8, 102.2, 98.4 ppm; MS (ESI): m/z 269 [M-H]⁻.

(Z)-2-(3-hydroxybenzylidene)-4,6-dihydroxybenzofuran-3(2H)-one (9c): The compound was prepared according to procedure B, starting from 4,6-dihydroxybenzofuran-3(2H)-one (4) and 3-hydroxybenzaldehyde, and was purified by column chromatography on silica gel eluted with CH₂Cl₂/MeOH (9:1) to yield a pure yellow solid (49%). M.p. > 230 °C (decomposition); ¹H NMR (400 MHz, [D₆]DMSO): δ = 11.03 (brs, 2H; OH), 9.63 (brs, 1H; OH), 7.28 (m, 3H; H2', H5', H6'), 6.80 (ddd, J_1 = 7.5 Hz, J_2 = 2.1 Hz, J_3 = 1.5 Hz, 1H; H4'), 6.49 (s, 1H; -CH=), 6.19 (d, J = 1.6 Hz, 1H; H7), 6.07 ppm (d, J = 1.6 Hz, 1H; H5); ¹³C NMR (100 MHz, [D₆]DMSO): δ = 179.0, 167.8, 167.6, 158.5, 157.5, 147.7, 133.4, 129.8, 121.9, 116.9, 116.5, 108.3, 102.5, 97.8, 90.5 ppm; MS (ESI): m/z 269 [M-H]⁻.

Enzymatic assays: *A. bisporus* TyM1 (6.4 mg; Sigma–Aldrich) was dissolved in phosphate buffer (5 mL, 50 mM, pH 7.0) and purified by Q-Sepharose FF chromatography with a NaCl gradient (0–1.0 M).^[24] The purity of tyrosinase was checked with SDS-PAGE (purified tyrosinase exhibits two bands: M_w ~14 and 45 kDa). Tyrosinase activity was measured spectroscopically with L-DOPA as the substrate. TyB3 was prepared from liquid cultures of *S. antibioticus* harboring the pIJ703 expression plasmid, and purified according to published procedures.^[21] Through all purification steps, protein solutions were kept on ice to prevent loss of enzymatic activity. The purity of the sample was indicated by the presence of a single band in the SDS-PAGE gel. All compounds were dissolved in 10% DMSO, and the DMSO stock solutions were diluted in phosphate buffer (pH 7.0). Tyrosinase (6 U) was preincubated with the compounds in phosphate buffer (50 mM, pH 7.0) for 5 min at 25 °C, then L-DOPA (2 mM) was added to the reaction mixture. The enzyme reaction was monitored by measuring the absorbance at 475 nm (DOPACHrome) for 5 min.

Computational methods: Calculations were performed with the recently resolved mushroom tyrosinase from *A. bisporus* (PDB ID: 2Y9X; TyM1)^[7] and the bacterial tyrosinase from *S. castaneoglobisporus* (PDB ID: 2AHK; TyB2).^[6] The initial PDB structures were solvated in a TIP3P water rectangular box (10 Å larger than the solute in every direction). All histidines were protonated. To construct the initial position of the aurone in the active Ty sites, we employed the optimized structures of TyM1 and TyB2 complexed with deprotonated HOPNO (2-hydroxypyridine-*N*-oxide), an efficient competitive inhibitor of TyM1^[31] and TyB3^[32] in a monodentate binding mode. As the enzymatic study^[22] demonstrate that aurones are more likely to interact with the active site at the B-ring, we aligned this ring with HOPNO by using the “pair fitting” tool of PYMOL.^[33] The 4'-hydroxy group of each aurone was superimposed on the oxygen atom of the NO group of HOPNO, linked to one copper atom of Ty.^[31,32] We considered the 4'-hydroxy group in its depro-

tonated form while the other hydroxy groups of the aurone were protonated. This hypothesis was tested, and the results are given in Supporting Information (Figures S3 and S4). Then, MM minimization with AMBER10 was carried out with the protein and the fixed ligand.^[34] For copper ions, histidine residues, and the hydroxyl group linked to the copper atoms in the active site, specific parameters were used.^[32] QM/MM calculations were performed with the Gaussian03 package^[35] for QM and with Tinker 4.2^[36] for MM. Both mechanical and electrostatic embedding (direct polarization) schemes were used to describe the interactions between the QM and the MM parts, thus ensuring a good description of the effects of the environment of the active site. The QM part contained the two coppers (in triplet state), the hydroxyl ion, the ligand, a water molecule close to the copper, the side chains of the six histidines linked to the coppers, and (for TyM1) Cys83, which forms a covalent thioether bond with His85. The rest of the protein and the solvent were computed at the MM level. The partition between QM and MM parts led to the cut of six or seven C α –C β bonds of the histidines (and of Cys83). The link atom scheme was used to treat the QM/MM boundary. The QM part was computed with the B3LYP/6-31G* level of theory and the MM part with Amber 99SB force-field parameters. Geometry optimizations were first performed only with residues at 4 Å of the QM part and allowed to move (other residues were frozen). Afterwards, QM/MM Born-Oppenheimer molecular dynamics were run in the NVT ensemble at 298 K by using the Berendsen algorithm. The time step was increased by using mass-scaling molecular dynamics. The hydrogen mass was set at 10 amu in order to “freeze” the X–H vibrations and allow us to employ of 3 fs time steps for the dynamics.^[37] For each complex, a 4 ps dynamic simulation was performed. After 1.5 ps of equilibration, ten snapshots were selected to calculate the binding affinities by using the QM/MM-PBSA approach (Equations (1) and (2)).

$$\Delta G = G_{\text{complex}} - G_{\text{protein}} - G_{\text{ligand}} \quad (1)$$

$$G(X) = E_{\text{QM/MM}}(X) + G_{\text{PB}}(X) + G_{\text{SA}}(X) \quad (2)$$

Having compared three structurally close ligands binding the same protein, changes in solute entropy were not included in the calculations. For the QM/MM scoring function, only the ligand was treated at the QM level. The PBSA part was computed with AMBER10. The charges used for these calculations were the charges of the Amber 99SB force field for the protein, the Mulliken charges for the coppers, and the hydroxyl ion obtained after our QM/MM simulations. For the ligands, charges were derived with a RESP fit on HF/6-31g* calculations.^[38] The decomposition of the QM/MM interaction in a van der Waals contribution and an electrostatic contribution are given in the Supporting Information (Tables S2 and S3).

Acknowledgements

The authors are grateful to ANR (Agence Nationale pour la Recherche) for financial support (Labex Arcane (ANR-11-LABX-0003-01) and Blanc program 2Cu-TargMelanin (ANR-09-BLAN-0028-01/02/03), CECIC for computer facilities and the European COST Program in the framework of which this work was carried out (COST action CM1003 WG 2). The work has been partially financed by the grant “Human recombinant tyrosinase: a testing bench for new drugs to treat melanin-related disorders” (Progetto di Ricerca di Ateneo CPDA110789/11) from the University of Padova to E.B.

Keywords: aurones · bacterial tyrosinases · enzymes · inhibitors · mushroom tyrosinases · QM/MM

- [1] C. Belle in *Encyclopedia of Metalloproteins* (Eds.: R. H. Kretsinger, V. N. Uversky, E. A. Permyakov), Springer, New York, **2013**, pp. 574–579.
- [2] E. I. Solomon, U. M. Sundaram, T. E. Machonkin, *Chem. Rev.* **1996**, *96*, 2563–2606.
- [3] M. Rolff, J. Schottenheim, H. Decker, F. Tuzcek, *Chem. Soc. Rev.* **2011**, *40*, 4077–4098.
- [4] P. M. Plonka, M. Grabacka, *Acta Biochim. Pol.* **2006**, *53*, 429–443.
- [5] M. Sendovski, M. Kanteev, V. S. Ben-Yosef, N. Adir, A. Fishman, *J. Mol. Biol.* **2011**, *405*, 227–237.
- [6] Y. Matoba, T. Kumagai, A. Yamamoto, H. Yoshitsu, M. Sugiyama, *J. Biol. Chem.* **2006**, *281*, 8981–8990.
- [7] W. T. Ismaya, H. J. Rozeboom, A. Weijin, J. J. Mes, F. Fusetti, H. J. Wichers, B. W. Dijkstra, *Biochemistry* **2011**, *50*, 5477–5486.
- [8] N. Fujieda, S. Yabuta, T. Ikeda, T. Oyama, N. Muraki, G. Kurisu, S. Itoh, *J. Biol. Chem.* **2013**, *288*, 22128–22140.
- [9] T.-S. Chang, *Int. J. Mol. Sci.* **2009**, *10*, 2440–2475.
- [10] K. R. Alexander, P. E. Kilbride, G. A. Fishman, M. Fishman, *Vision Res.* **1987**, *27*, 1077–1083.
- [11] K. Kalinderi, L. Fidani, Z. Katsarou, S. Bostantjopoulou, *Int. J. Clin. Pract.* **2011**, *65*, 1289–1294.
- [12] J. M. Gillbro, M. J. Olsson, *Int. J. Cosmet. Sci.* **2011**, *33*, 210–221.
- [13] N. Smit, J. Vicanova, S. Pavel, *Int. J. Mol. Sci.* **2009**, *10*, 5326–5349.
- [14] M. Friedman, *J. Agric. Food Chem.* **1996**, *44*, 631–653.
- [15] M. R. Loizzo, R. Tundis, R. Menichini, *Compr. Rev. Food Sci. Food Saf.* **2012**, *11*, 378–398.
- [16] T. F. M. Kuijpers, H. Gruppen, S. Sforza, W. J. H. van Berkel, J.-P. Vincken, *FEBS J.* **2013**, *280*, 6184–6195.
- [17] T. F. M. Kuijpers, T. van Herk, J.-P. Vincken, R. H. Janssen, D. L. Narh, W. J. H. van Berkel, H. Gruppen, *J. Agric. Food Chem.* **2014**, *62*, 214–221.
- [18] S. Okombi, D. Rival, S. Bonnet, A.-M. Mariotte, E. Perrier, A. Boumendjel, *J. Med. Chem.* **2006**, *49*, 329–333.
- [19] a) A. Boumendjel, *Curr. Med. Chem.* **2003**, *10*, 2621–2630; b) C. Zwergel, F. Gaascht, S. Valente, M. Diederich, D. Bagrel, G. Kirsch, *Nat. Prod. Commun.* **2012**, *7*, 389–394; c) R. Haudecoeur, A. Boumendjel, *Curr. Med. Chem.* **2012**, *19*, 2861–2875.
- [20] a) R. Haudecoeur, A. Ahmed-Belkacem, W. Yi, A. Fortuné, R. Brillet, C. Belle, E. Nicolle, C. Pallier, J.-M. Pawlotsky, A. Boumendjel, *J. Med. Chem.* **2011**, *54*, 5395–5402; b) H. Cheng, L. Zheng, Y. Liu, S. Chen, X. Cheng, X. Lu, Z. Zheng, G.-C. Zhou, *Eur. J. Med. Chem.* **2010**, *45*, 5950–5957; c) C.-Y. Lee, E.-H. Chew, M.-L. Go, *Eur. J. Med. Chem.* **2010**, *45*, 2957–2971; d) H.-M. Sim, C.-P. Wu, S. V. Ambudkar, M.-L. Go, *Biochem. Pharmacol.* **2011**, *82*, 1562–1571; e) B. P. Bandgar, S. A. Patil, B. L. Korbadi, S. C. Biradar, S. N. Nile, C. N. Khobragade, *Eur. J. Med. Chem.* **2010**, *45*, 3223–3227; f) K. N. Tiwari, J.-P. Monserrat, A. Hequet, C. Ganem-Elbaz, T. Cresteil, G. Jaouen, A. Vessières, E. A. Hillard, C. Jolivald, *Dalton Trans.* **2012**, *41*, 6451–6457; g) M. Roussaki, S. Costa Lima, A.-M. Kypreou, P. Kefalas, A. Cordeiro da Silva, A. Detsi, *Int. J. Med. Chem.* **2012**, *2012*, 196921; h) S. Y. Shin, M. C. Shin, J.-S. Shin, K.-T. Lee, Y. S. Lee, *Bioorg. Med. Chem. Lett.* **2011**, *21*, 4520–4523; i) M. Ono, R. Ikeoka, H. Watanabe, H. Kimura, T. Fuchigami, M. Haratake, H. Saji, M. Nakayama, *Bioorg. Med. Chem. Lett.* **2010**, *20*, 5743–5748; j) S. Shrestha, S. Natarajan, J.-H. Park, D.-Y. Lee, J.-G. Cho, G.-S. Kim, Y.-J. Jeon, S.-W. Yeon, D.-C. Yang, N.-I. Baek, *Bioorg. Med. Chem. Lett.* **2013**, *23*, 5150–5154.
- [21] L. Bubacco, M. van Gastel, E. J. J. Groenen, E. Vijgenboom, G. W. Canters, *J. Biol. Chem.* **2003**, *278*, 7381–7389.
- [22] C. Dubois, R. Haudecoeur, M. Orio, C. Belle, C. Bochot, A. Boumendjel, R. Hardré, H. Jamet, M. Réglie, *ChemBioChem* **2012**, *13*, 559–565.
- [23] M. R. L. Stratford, C. A. Ramsden, P. A. Riley, *Bioorg. Med. Chem.* **2013**, *21*, 1166–1173.
- [24] S. Yamazaki, S. Itoh, *J. Am. Chem. Soc.* **2003**, *125*, 13034–13035.
- [25] Z. Yang, F. Wu, *Biotechnology* **2006**, *5*, 344–348.
- [26] A. Cornish-Bowden, *Fundamentals of Enzyme Kinetics*, Portland, London, **1995**.
- [27] P. A. Kollman, I. Massova, C. Reyes, B. Kuhn, S. Huo, L. Chong, M. Lee, T. Lee, Y. Duan, W. Wang, O. Donini, P. Cieplak, J. Srinivasan, D. A. Case, T. E. Cheatham, *Acc. Chem. Res.* **2000**, *33*, 889–897.
- [28] A. Ciancetta, S. Genheden, U. Ryde, *J. Comput.-Aided Mol. Des.* **2011**, *25*, 729–742.
- [29] M. Retegan, A. Milet, H. Jamet, *J. Chem. Inf. Model.* **2009**, *49*, 963–971.
- [30] S. Takahashi, T. Kamiya, K. Saeki, T. Nezu, S.-i. Takeuchi, R. Takasawa, S. Sunaga, A. Yoshimori, S. Ebikura, T. Abe, S.-i. Tanuma, *Bioorg. Med. Chem.* **2010**, *18*, 8112–8118.
- [31] E. Peyroux, W. Ghattas, R. Hardré, M. Giorgi, B. Faure, A. J. Simaan, C. Belle, M. Réglie, *Inorg. Chem.* **2009**, *48*, 10874–10876.
- [32] C. Bochot, E. Favre, C. Dubois, B. Baptiste, L. Bubacco, P.-A. Carrupt, G. Gellon, R. Hardré, D. Luneau, Y. Moreau, A. Nurisso, M. Réglie, G. Serratrice, C. Belle, H. Jamet, *Chem. Eur. J.* **2013**, *19*, 3655–3664.
- [33] W. Delano, *The PyMOL Molecular Graphics System*, DeLano Scientific, Palo Alto, CA, **2006**.
- [34] D. A. Case, T. A. Darden, T. E. Cheatham III, C. L. Simmerling, J. Wang, R. E. Duke, R. Luo, M. Crowley, R. C. Walker, W. Zhang, K. M. Merz, B. Wang, S. Hayik, A. Roitberg, G. Seabra, I. Kolossváry, K. F. Wong, F. Paesani, J. Vanicek, X. Wu, S. R. Brozell, T. Steinbrecher, H. Gohlke, L. Yang, C. Tan, J. Mongan, V. Hornak, G. Cui, D. H. Mathews, M. G. Seetin, C. Sagui, V. Babin, P. A. Kollman, *AMBER 10*, University of California, San Francisco, **2008**.
- [35] M. J. Frisch, G. W. Trucks, H. B. Schlegel, G. E. Scuseria, M. A. Robb, J. R. Cheeseman, J. A. Montgomery Jr., T. Vreven, K. N. Kudin, J. C. Burant, J. M. Millam, S. S. Iyengar, J. Tomasi, V. Barone, B. Mennucci, M. Cossi, G. Scalmani, N. Rega, G. A. Petersson, H. Nakatsuji, M. Hada, M. Ehara, K. Toyota, R. Fukuda, J. Hasegawa, M. Ishida, T. Nakajima, Y. Honda, O. Kitao, H. Nakai, M. Klene, X. Li, J. E. Knox, H. P. Hratchian, J. B. Cross, V. Bakken, C. Adamo, J. Jaramillo, R. Gomperts, R. E. Stratmann, O. Yazyev, A. J. Austin, R. Cammi, C. Pomelli, J. W. Ochterski, P. Y. Ayala, K. Morokuma, G. A. Voth, P. Salvador, J. J. Dannenberg, V. G. Zakrzewski, S. Dapprich, A. D. Daniels, M. C. Strain, O. Farkas, D. K. Malick, A. D. Rabuck, K. Raghavachari, J. B. Foresman, J. V. Ortiz, Q. Cui, A. G. Baboul, S. Clifford, J. Cioslowski, B. B. Stefanov, G. Liu, A. Liashenko, P. Piskorz, I. Komaromi, R. L. Martin, D. J. Fox, T. Keith, M. A. Al-Laham, C. Y. Peng, A. Nanayakkara, M. Challacombe, P. M. W. Gill, B. Johnson, W. Chen, M. W. Wong, C. Gonzalez, J. A. Pople, *Gaussian 03*, Revision A1, Gaussian, Inc., Wallingford CT, **2004**.
- [36] J. W. Ponder, *Tinker 4.2 ed.*, Washington University, Saint Louis, **2004**.
- [37] H. Zheng, S. Wang, Y. Zhang, *J. Comput. Chem.* **2009**, *30*, 2706–2711.
- [38] W. D. Cornell, P. Cieplak, C. I. Bayly, P. A. Kollman, *J. Am. Chem. Soc.* **1993**, *115*, 9620–9631.

Received: February 3, 2014

Published online on ■■■■■, 0000

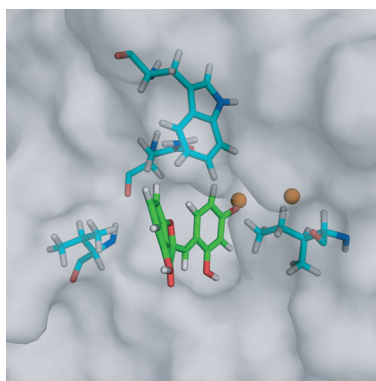
FULL PAPERS

R. Haudecoeur, A. Gouron,
A. Boumendjel*

■■■ – ■■■



**Investigation of Binding-Site
Homology between Mushroom and
Bacterial Tyrosinases by Using
Aurones as Effectors**



A lighter future: Aurones have been identified as inhibitors of melanin biosynthesis. In this study, 24 aurones were evaluated on mushroom and bacterial tyrosinases (TyM and TyB). The compounds behaved as inhibitors, substrates, or activators of both enzymes. Our results highlight similarities and differences in behavior between TyM and TyB with the same set of molecules.